Development and Application of a Novel Class of Hierarchical Tangential Vector Finite Elements for Electromagnetics

Lars S. Andersen, *Student Member, IEEE,* and John L. Volakis, *Fellow, IEEE*

***Abstract*—Tangential vector finite elements (TVFE's) overcome most of the shortcomings of node-based finite elements for electromagnetic simulations. For a triangular element, this paper proposes a class of hierarchical TVFE's that differ from traditional TVFE's. The hierarchical nature of the proposed TVFE's makes them ideally suited for employing an efficient selective field expansion (the lowest order TVFE employed within part of the computational domain and a higher order TVFE employed within the remaining part of the computational domain). This is an attractive feature not shared by nonhierarchical TVFE's for which a more traditional approach (the same TVFE employed throughout the computational domain) must be applied. For determining the scattering by composite cylinders, this paper argues that the performance (in terms of accuracy, memory, and, in most cases, CPU time) of the proposed class of hierarchical TVFE's when applying selective field expansion is superior to that of the lowest order TVFE and a traditional nonhierarchical TVFE. This is the case when an artificial absorber as well as a boundary integral is used for truncating the computational domain. A guideline is given as to how lowest and higher order TVFE's shall be combined for optimal performance of the proposed class of hierarchical TVFE's.**

***Index Terms*— Edge-based elements, electromagnetic fields, finite-element methods.**

I. Introduction

NODE-BASED expansions in finite-element method (FEM) solutions are suitable for modeling scalar quantities, but typically not so for simulating vector electromagnetic fields. When assigning vector field values to element nodes, values may need to be specified at locations where the true field is undefined (corners, edges), spurious modes can be generated, and the enforcement of the boundary conditions occurring in electromagnetics can be a challenging task. Tangential vector finite elements (TVFE's), based on expanding a vector field in terms of values associated with element edges and faces, have been shown to be free of these shortcomings [1] and, therefore, TVFE's are of considerable practical interest.

A TVFE is referred to as polynomial-complete to a given order, say n, if all possible polynomial variations up to and including order n are captured within the element and on the element boundary. For a triangular element, polynomial-complete expansion to order n requires $(n+1)(n+2)$ vector basis functions. Nédélec pointed out [2], [3] that it is not necessarily advantageous to employ polynomial-complete TVFE's when applying the FEM. It was proven that a polynomial-complete expansion of a vector field $\mathbf{A}$ can be decomposed into a part representing the range space of the curl operator ($\nabla \times \mathbf{A} \neq 0$, $\mathbf{A} \neq \nabla\phi$) and a part representing the null space of the curl operator ($\nabla \times \mathbf{A} = 0$, $\mathbf{A} = \nabla\phi$). For representation of electromagnetic fields, it suffices to employ a TVFE that is complete in the range space of the curl operator. Since such a TVFE captures polynomial variations of order n interior to the element and polynomial variations of order $n-1$ along element edges, we call it complete to order $n-0.5$ and refer to it as a mixed-order TVFE or (less commonly) a reduced-order TVFE. For a triangular element, complete expansion to order $n-0.5$ requires $n(n+2)$ vector basis functions. For rigorous criteria for spurious mode elimination and extensive discussions of mixed-order TVFE's versus polynomial-complete TVFE's, see [2] and [3]. For discussions of element completeness and spurious modes, see also [4]–[7].

A class of TVFE's is referred to as hierarchical if the vector basis functions forming the nth order TVFE are a subset of the vector basis functions forming the $(n+1)$th order TVFE. This desirable property allows for selective field expansion using different order TVFE's in different regions of the computational domain. Hence, lowest order TVFE's can be employed in regions where the field is expected to vary slowly whereas higher order TVFE's can be employed in regions where rapid field variation is anticipated. This selective choice of TVFE's over the computational domain can lead to a memory and CPU time reduction as well as improved accuracy. Scalar FEM analysis using hierarchical finite elements is a well-known approach (see, for example, [8] and [9]).

For a triangular element, the lowest order TVFE was originally introduced by Whitney [10] and is referred to as the Whitney TVFE or the Whitney element. It provides a constant tangential field value along element edges and a linear field variation inside the element. Hence, the Whitney TVFE is complete to order 0.5. Several nonhierarchical TVFE's of higher order than the Whitney TVFE have been introduced by Mur and de Hoop [11], Lee *et al.* [12], Peterson [13], Peterson and Wilton [5], and Graglia *et al.* [14]. Recently, Carrié and Webb [15] presented a hierarchical TVFE derived directly from a set of scalar finite-element basis functions [9]. A hierarchical TVFE for a tetrahedral element (the special

Manuscript received September 8, 1997; revised July 15, 1998.

The authors are with the Radiation Laboratory, Department of Electrical Engineering and Computer Science, University of Michigan, Ann Arbor, MI 48109 USA.

Publisher Item Identifier S 0018-926X(99)02204-8.

case of a triangular element follows trivially from the case of a tetrahedral element) up to and including second order was introduced by Webb and Forghani [16]. A recent review of TVFE's was given by Peterson and Wilton [7].

The discussion above presents the concepts of polynomial-complete, mixed-order, and hierarchical TVFE's and summarizes different TVFE's that have been proposed for a triangular element. However, there still seems to be a need for thorough numerical investigations of the effectiveness (in terms of accuracy and time/memory requirements) of selective field expansion using hierarchical TVFE's. The purpose of this paper is to introduce a class of hierarchical mixed-order TVFE's for a triangular element and to demonstrate its performance when a selective field expansion is employed. The hierarchical TVFE's differ from those previously presented for a triangular element. The derivation is based on an attractive set of higher order vector basis functions recently presented by Popović and Kolundžija [17], [18] for expanding surface currents in conjunction with method of moments (MoM) solutions. These are converted to vector basis functions applicable for FEM analysis and knowledge of Nédélec spaces and traditional nonhierarchical mixed-order TVFE's is then applied to specifically propose hierarchical mixed-order TVFE's of order 0.5, 1.5, and 2.5. Potentially, even higher order hierarchical mixed-order TVFE's can be formulated. We demonstrate the performance of the proposed class of hierarchical TVFE's by comparing FEM results obtained using the Whitney TVFE and the proposed hierarchical TVFE's (applying a selective field expansion) to MoM solutions.

The structure of this paper is as follows. Section II presents the derivation of vector basis functions based on the expansion introduced by Popović and Kolundžija. Section III discusses the merits of the proposed vector basis functions and proposes hierarchical mixed-order TVFE's that are compared to existing mixed-order TVFE's. Expressions in terms of simplex coordinates are given and vector plots are added to provide a physical understanding of the TVFE's. Section IV presents a set of numerical results that demonstrate the performance of the proposed class of hierarchical TVFE's. Section V summarizes and concludes the paper and outlines future work to be carried out. Parts of this work were presented earlier [19].

II. Formulation

The proposed class of hierarchical TVFE's is based on an expansion introduced by Popović and Kolundžija [17], [18] for the surface current on a perfectly electrically conducting (PEC) generalized quadrilateral. For this expansion, it is demonstrated in [17] and [18] that the surface current can be expanded using approximately ten unknowns per square wavelength as opposed to approximately one hundred unknowns per square wavelength for traditional subdomain pulse-basis functions. This suggests that the expansion introduced by Popović and Kolundžija is very efficient. Below, corresponding vector basis functions applicable for FEM analysis are constructed.

As a degenerate case of the generalized quadrilateral considered in [17] and [18], we consider a triangular element with nodes 1–3 described by position vectors $\mathbf{r}_1$, $\mathbf{r}_2$, and $\mathbf{r}_3$ with respect to the origin O of a rectangular coordinate system (see Fig. 1). The edges from node 1 to node 2, node 2 to node 3 and node 3 to node 1 are referred to as edge #1, edge #2, and edge #3, respectively. The area of the triangle is denoted by A. Simplex (or area) coordinates ζ_1, ζ_2, and ζ_3 at a point P described uniquely by a position vector $\mathbf{r}$ are defined in the usual manner, *viz.* $\zeta_n = A_n/A$ where A_n denotes the area of the triangle formed by P and the endpoints of the edge opposite to node n. We let $\hat{n}$ denote a unit normal vector to the surface of the triangle.

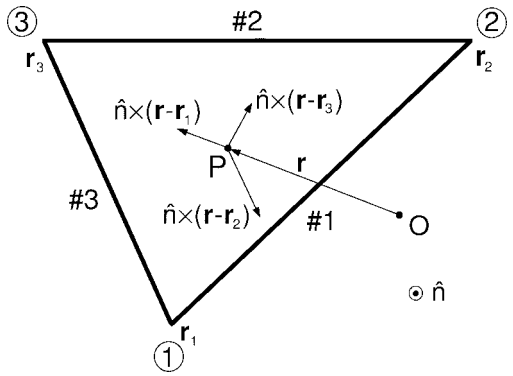

Fig. 1. Geometry of a triangular element and illustration of the vectors $\hat{n} \times (\mathbf{r} - \mathbf{r}_n)$, $n = 1, 2, 3$, describing the directions of the vector basis functions at the point P.

Popović and Kolundžija expands the surface current $\mathbf{J}_s$ over the triangle as [17]

$$\mathbf{J}_s = \sum_{n=1}^{3} \mathbf{J}_{sn} = \sum_{n=1}^{3} \Psi_n \mathbf{V}_n \tag{1}$$

where

$$\mathbf{V}_n = \frac{\mathbf{r} - \mathbf{r}_n}{2A} \tag{2}$$

is a vector whose direction is from node n to P and Ψ_n is a polynomial function of position that provides the amplitude variation of the vector current component $\mathbf{J}_{sn} = \Psi_n \mathbf{V}_n$. The polynomial Ψ_n contains a number of unknown expansion coefficients. Its specific form is irrelevant at this point and will be given later. As in the Rao–Wilton–Glisson expansion [20], $\mathbf{J}_{sn}$ has no normal component along the two edges sharing node n and $\mathbf{J}_{sn}$ has both a normal and a tangential component along the edge opposite to node n. Thus, the quantity

$$\begin{aligned} \mathbf{F}_n &= \hat{n} \times \mathbf{J}_{sn} = \Psi_n \hat{n} \times \mathbf{V}_n \\ &= \Psi_n \frac{\hat{n} \times (\mathbf{r} - \mathbf{r}_n)}{2A} = \Psi_n \mathbf{W}_n \end{aligned} \tag{3}$$

with

$$\mathbf{W}_n = \frac{\hat{n} \times (\mathbf{r} - \mathbf{r}_n)}{2A} \tag{4}$$

has no tangential component along the two edges sharing node n and has both a tangential and a normal component along the edge opposite to node n. This suggests that the vector basis functions multiplying the expansion coefficients in the expansion of $\mathbf{F}_n$ can be employed as vector basis functions for the edge opposite to node n when applying the

FEM. Considering all three edges, the FEM expansion of an unknown vector quantity $\mathbf{F}$ becomes

$$\mathbf{F} = \hat{n} \times \mathbf{J}_s = \sum_{n=1}^{3} \hat{n} \times \mathbf{J}_{sn} = \sum_{n=1}^{3} \mathbf{F}_n = \sum_{n=1}^{3} \Psi_n \mathbf{W}_n \quad (5)$$

where expressions for Ψ_n (depending upon the order of the expansion) and $\mathbf{W}_n$ (independent of the order of the expansion) are to be presented.

Introducing coordinates over the triangle and using relations from [17], it is shown in Appendix A that

$$\mathbf{W}_1 = \zeta_2 \nabla \zeta_3 - \zeta_3 \nabla \zeta_2 \quad (6)$$

$$\mathbf{W}_2 = \zeta_3 \nabla \zeta_1 - \zeta_1 \nabla \zeta_3 \quad (7)$$

$$\mathbf{W}_3 = \zeta_1 \nabla \zeta_2 - \zeta_2 \nabla \zeta_1. \quad (8)$$

The polynomial Ψ_n is a function of position that in terms of a number of unknown expansion coefficients provides the amplitude variation of the vector component $\mathbf{W}_n$. It can be defined using normalized coordinates u_n and v_n over the triangle. Specifically, we choose $u_n = 0$ at node n, $u_n = 1$ along the edge opposite to node n and $v_n = \pm 1$ along the two edges sharing node n. A detailed description of the variation of u_n and v_n is given in Appendix A. From [17], we have

$$\Psi_n = 2 \sum_{j=1}^{n_v} \left[b_n^j + \sum_{i=3}^{n_u} a_n^{ij} (u_n^{i-2} - 1) \right] v_n^{j-1} \quad (9)$$

where n_v and n_u are integer constants determining the order of the approximation and b_n^j and a_n^{ij} are the expansion coefficients. Also, $u_1 = \zeta_2 + \zeta_3$, $u_1 v_1 = \zeta_2 - \zeta_3$, $u_2 = \zeta_3 + \zeta_1$, $u_2 v_2 = \zeta_3 - \zeta_1$, $u_3 = \zeta_1 + \zeta_2$, and $u_3 v_3 = \zeta_1 - \zeta_2$.

Expansion (5) for $\mathbf{F}$ along with (6)–(8) for $\mathbf{W}_1$, $\mathbf{W}_2$, and $\mathbf{W}_3$ and (9) for Ψ_n describes the proposed vector basis functions. However, a certain simplification provides a more familiar form. By regrouping the terms in (9) for Ψ_n, (5) for $\mathbf{F}$ can be cast into

$$\mathbf{F} = \sum_{k=1}^{3} \sum_{m=1}^{N^{n_v n_u}} c_{k,m}^{n_v n_u} \mathbf{W}_{k,m}^{n_v n_u} \quad (10)$$

where $N^{n_v n_u} = n_v(n_u - 1)$ denotes the total number of vector basis functions per edge for the given values of n_u and n_v. Also, $c_{k,m}^{n_v n_u}$ are expansion coefficients corresponding to edge $\#k$ while $\mathbf{W}_{k,m}^{n_v n_u}$ are vector basis functions associated with edge $\#k$. $\mathbf{W}_{k,m}^{n_v n_u}$ is given (in terms of the simplex coordinates ζ_1, ζ_2, and ζ_3) as a function of ζ_1, ζ_2, and ζ_3 times a direction vector ($\zeta_1 \nabla \zeta_2 - \zeta_2 \nabla \zeta_1$ for $k = 1$, $\zeta_2 \nabla \zeta_3 - \zeta_3 \nabla \zeta_2$ for $k = 2$ and $\zeta_3 \nabla \zeta_1 - \zeta_1 \nabla \zeta_3$ for $k = 3$). Except for normalization constants, the vector basis functions $\mathbf{W}_{k,m}^{n_v n_u}$ will be directly used for forming hierarchical mixed-order TVFE's (see Section III).

III. Discussion

In this section, we examine the properties of the vector basis functions introduced in the previous section and based on these we propose new hierarchical mixed-order TVFE's that are contrasted to existing mixed-order TVFE's.

From (10), we recover for $(n_v, n_u) = (1, 2)$ the three vector basis functions introduced by Whitney [10]. For larger values of n_v and n_u, (10) includes additional vector basis functions all of which maintain the same fundamental direction vectors ($\zeta_1 \nabla \zeta_2 - \zeta_2 \nabla \zeta_1$ for edge $\#1$, $\zeta_2 \nabla \zeta_3 - \zeta_3 \nabla \zeta_2$ for edge $\#2$, and $\zeta_3 \nabla \zeta_1 - \zeta_1 \nabla \zeta_3$ for edge $\#3$). Thus, the proposed higher order vector basis functions differ from the lowest order vector basis functions only in magnitude and, hence, in a given point of the triangle, the field expanded using a TVFE based on these vector basis functions is represented as a linear combination of vector basis functions having only three fundamental directions. This is one of the major differences between the proposed and traditional hierarchical TVFE's [15], [16]. For the latter, the higher order vector basis functions differ from the lowest order vector basis functions in both magnitude and direction. The field in a given point of the triangle is again represented as a linear combination of vector basis functions, but in this case, the number of fundamental vector directions used for representing the field grows with the order of the TVFE.

An important property of (10) is that the vector basis functions $\mathbf{W}_{k,m}^{n_v n_u}$ for $k = 1, 2, 3$ and $m = 1, \cdots, N^{n_v n_u}$ are a subset of the vector basis functions $\mathbf{W}_{k,m}^{(n_v+1)(n_u+1)}$ for $k = 1, 2, 3$ and $m = 1, \cdots, N^{(n_v+1)(n_u+1)}$. This shows that TVFE's based on the above presented vector basis functions are hierarchical, a very desirable property. Hierarchical TVFE's are ideally suited for employing an efficient selective field expansion where different order TVFE's (in this case different values of n_v and n_u) are employed in different regions of the computational domain. Hence, for a uniform mesh, the lowest order TVFE can be employed in regions where the field is expected to experience smooth variation (regions where the relative material parameters are (nearly) unity, away from edges, etc.) whereas a higher order TVFE can be employed in regions where the field is expected to vary rapidly (near edges, close to material boundaries, in dense materials, etc.). Similarly, for a nonuniform mesh (for example, where geometric complexity requires detailed meshing in a given region), the lowest order TVFE can be employed where the mesh is dense while a higher order TVFE can be employed where the mesh is coarse. Regions where higher order TVFE's are employed can be fixed *a priori* or an adaptive scheme can be developed where lowest order TVFE's are initially employed throughout the computational domain and higher order TVFE's are subsequently employed in regions where the error is estimated to be large.

Based on the vector basis functions in (10) for different values of n_v and n_u along with knowledge of Nédélec spaces and traditional nonhierarchical mixed-order TVFE's, hierarchical mixed-order TVFE's of order 0.5, 1.5, and 2.5 will now be proposed and compared to existing TVFE's. The method has the potential of providing hierarchical mixed-order TVFE's of even higher orders if so desired. Explicit expressions for vector basis functions are given in Appendix B.

For the special case of $(n_v, n_u) = (1, 2)$, we obtain from (10) a set of three vector basis functions $\mathbf{W}_{k,1}^{12}$, $k = 1, 2, 3$, forming a mixed-order TVFE of order 0.5 identical to the Whitney TVFE [10] (see Appendix B). This result was expected since the lowest order expansion adopted by Popović

and Kolundžija is identical to the Rao–Wilton–Glisson expansion [20] whose vector basis functions reduce to the Whitney vector basis functions when converted using the procedure applied above. This lowest order TVFE provides a constant tangential field along element edges, a linear variation of the normal field component along element edges (referred to as CT/LN field variation along element edges) and a linear field variation interior to the element.

A traditional second-order polynomial-complete TVFE is described by twelve vector basis functions (see [5]). However, by excluding the four vector basis functions associated with the null space of the curl operator, this second-order polynomial-complete TVFE can be reduced to a mixed-order TVFE of order 1.5 formed by eight vector basis functions as presented by Peterson [13] (see Appendix B). The latter provides a linear variation of the tangential field component along element edges, a quadratic variation of the normal field component along element edges (referred to as LT/QN field variation along element edges) and quadratic field variation interior to the element. Based on the vector basis functions from (10) for $(n_v, n_u) = (2, 3)$, we propose eight vector basis functions forming an alternative and hierarchical mixed-order TVFE of order 1.5 providing LT/QN field variation along element edges and quadratic field variation interior to the element (see Appendix B).

Peterson's mixed-order TVFE of order 1.5 [13] has the desirable property of being complete to second order in the range space of the curl operator. This property ensures a complete second-order expansion of a field with nonzero curl and guarantees eigenvalue solutions free of spurious nonzero eigenvalues. Due to the existence of a linear transformation (see Appendix B) from Peterson's eight vector basis functions to the proposed eight vector basis functions, the proposed hierarchical mixed-order TVFE of order 1.5 has the same desirable property. However, the two TVFE's are not identical. Their vector basis functions span the same space but have different properties and may not be equally efficient numerically.

For both mixed-order TVFE's of order 1.5, six of the vector basis functions provide a linearly varying tangential component along element edges while the remaining two vector basis functions (identical for the two different TVFE's) provide a quadratic variation of the normal field component along element edges. However, the linear variation of the tangential component along element edges is obtained in two different ways. For Peterson's mixed-order TVFE, the two unknowns per edge represent the magnitude of the field at edge endpoints. For the proposed mixed-order TVFE, the two unknowns per edge represent the average field value along the edge and the deviation from this average value at edge endpoints.

A generalization to even higher order hierarchical mixed-order TVFE's is possible. For the special case of $(n_v, n_u) = (3, 4)$, (10) gives vector basis functions that based on knowledge of Nédélec spaces and traditional nonhierarchical mixed-order TVFE's of order 2.5 [5], [21][1] can be used for forming a hierarchical mixed-order TVFE of order 2.5 (see Appendix B).

[1] A correction of the mixed-order TVFE of order 2.5 presented by Peterson and Wilton [5] was given by Peterson [21].

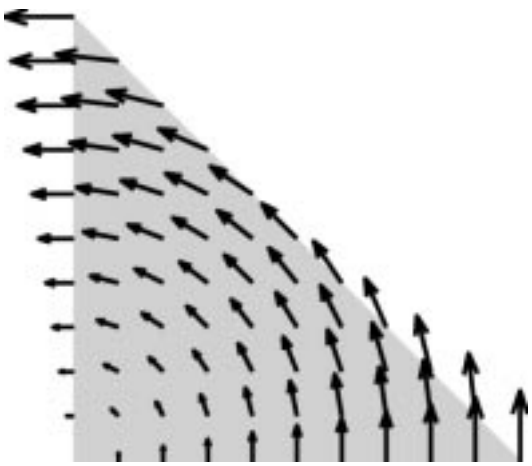

Fig. 2. Plot of the proposed vector basis function $\zeta_2\nabla\zeta_3 - \zeta_3\nabla\zeta_2$ for a triangular element.

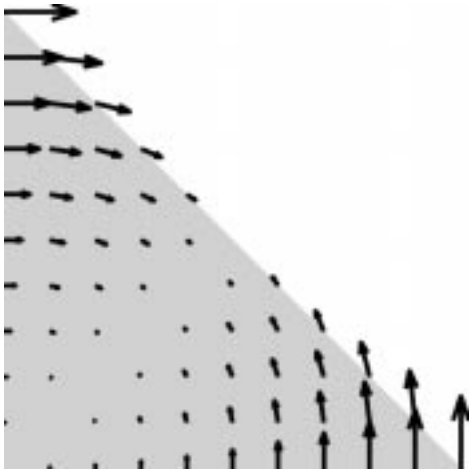

Fig. 3. Plot of the proposed vector basis function $(\zeta_2-\zeta_3)(\zeta_2\nabla\zeta_3-\zeta_3\nabla\zeta_2)$ for a triangular element.

The similarity between the hierarchical mixed-order TVFE's of order 1.5 and 2.5 is apparent and one gets an impression of the needed generalizations for obtaining even higher order TVFE's. However, use of TVFE's beyond order 2.5 does not seem to be of practical interest.

To pictorially illustrate the behavior of the proposed vector basis functions, we consider a triangular element where the nodes 1, 2, and 3 have the coordinates $(0, 0)$, $(1, 0)$, and $(0, 1)$ in a rectangular (x, y) coordinate system. The lowest order vector basis function $\zeta_2\nabla\zeta_3 - \zeta_3\nabla\zeta_2$ associated with edge $\#2$ is plotted in Fig. 2. For the proposed mixed-order TVFE of order 1.5, the linear variation of the tangential field along edge $\#2$ is provided by $\zeta_2\nabla\zeta_3 - \zeta_3\nabla\zeta_2$ (due to the hierarchical nature of the proposed class of TVFE's) and by $(\zeta_2 - \zeta_3)(\zeta_2\nabla\zeta_3 - \zeta_3\nabla\zeta_2)$ plotted in Fig. 3. For Peterson's mixed-order TVFE of order 1.5, the linear variation of the tangential field along edge $\#2$ is provided by $\zeta_2\nabla\zeta_3$ and by $\zeta_3\nabla\zeta_2$ individually (see Figs. 4 and 5) and this mixed-order TVFE, therefore, does not compare to the lowest order TVFE in a hierarchical fashion. The two vector basis functions providing quadratic normal field variation along element edges are the same for the two mixed-order TVFE's. The vector

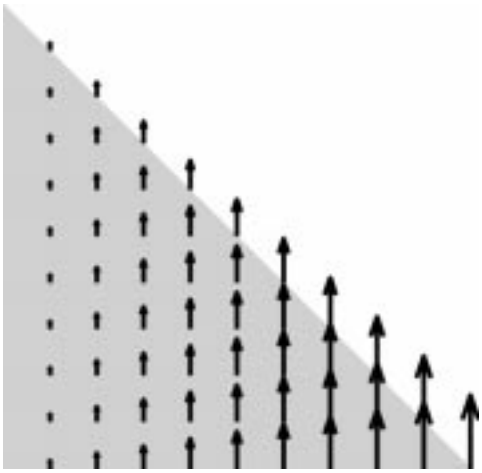

Fig. 4. Plot of the traditional vector basis function $\zeta_2 \nabla \zeta_3$ for a triangular element.

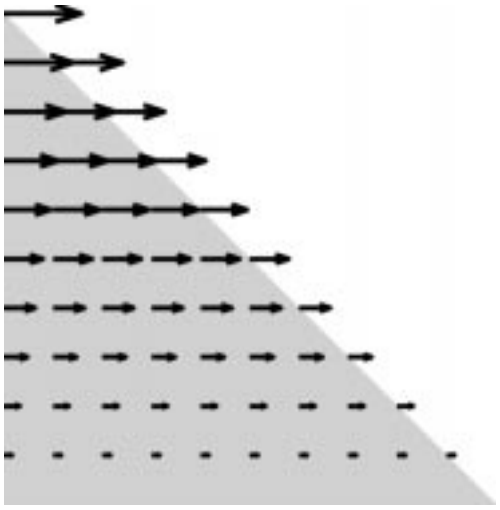

Fig. 5. Plot of the traditional vector basis function $\zeta_3 \nabla \zeta_2$ for a triangular element.

basis function $\zeta_1(\zeta_2 \nabla \zeta_3 - \zeta_3 \nabla \zeta_2)$ associated with edge #2 (zero field along edge #2) is plotted in Fig 6. All vector basis functions are seen to provide the postulated variation.

IV. Numerical Results

In the previous section, properties of various TVFE's were examined. Specifically, the mixed-order TVFE of order 0.5 (corresponding to $(n_v, n_u) = (1, 2)$, see also [10]), Peterson's mixed-order TVFE of order 1.5 [13] and the proposed hierarchical mixed-order TVFE of order 1.5 (corresponding to $(n_v, n_u) = (2, 3)$ and reduced from twelve to eight vector basis functions) were compared. It is the aim of this section to numerically demonstrate the performance of the proposed class of hierarchical TVFE's when the field is selectively expanded using the lowest order TVFE in part of the computational domain and the proposed hierarchical mixed-order TVFE of order 1.5 in the remaining part of the computational domain. A guideline will be given as to how lowest and higher order TVFE's shall be combined for optimal (with respect to accuracy, memory, and CPU time) performance.

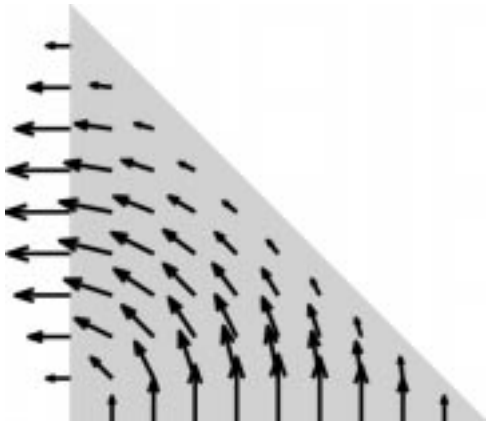

Fig. 6. Plot of the vector basis function $\zeta_1(\zeta_2 \nabla \zeta_3 - \zeta_3 \nabla \zeta_2)$ for a triangular element.

A FEM computer code was developed to evaluate the scattering of a TE or TM polarized plane wave by an arbitrary infinite cylinder composed of PEC's and isotropic dielectric and/or magnetic materials. The code is based on a standard FEM formulation for two-dimensional problems where the transverse field component is expanded using a TVFE and the solution domain is truncated using a homogeneous isotropic artificial absorber (AA) (a fictitious material of relative permittivity and permeability $1 - j2.7$ backed by a PEC structure) of thickness $0.25\lambda_0$ (λ_0 denotes the free-space wavelength) placed a distance $0.5\lambda_0$ from the scatterer [22]. The resulting sparse FEM matrix equation system is solved using a quasi-minimal residual solver [23]. For validation, MoM results were successfully compared to FEM results using each of the three TVFE's individually as well as the two different TVFE's selectively over the computational domain.

Let us consider a square PEC cylinder of side length λ_0 situated in a free space region characterized by the permittivity ε_0 and the permeability μ_0. Centered on the upper side of the cylinder is a rectangular groove of length $\lambda_0/2$ and of height $\lambda_0/4$. The groove is filled with a material characterized by the relative permittivity $\varepsilon_r = 2 - j2$ and the relative permeability $\mu_r = 2 - j2$. The cylinder is illuminated by a TE (with respect to the cylinder axis) polarized homogeneous plane wave whose propagation vector forms a 45° angle with all sides of the cylinder, as illustrated in Fig. 7.

In the following, we compare the scattering by the cylinder using different TVFE options and different uniform discretizations to demonstrate the merits of the proposed hierarchical mixed-order TVFE's when the field is selectively expanded over the computational domain. In Fig. 8, we compare results for the two-dimensional radar cross section (RCS) σ_{2-D} normalized to λ_0 as a function of the observation angle ϕ[2]. The MoM result is denoted "MoM." For a mesh where the generic element edge size is $0.15\lambda_0$, the FEM result using the lowest order TVFE is denoted "FEM-1 TVFE-coarse" and the FEM result using selective field expansion (with the groove and a layer surrounding the scatterer as the region in which the mixed-order TVFE of order 1.5 is employed)

[2] $\phi = 45°$ corresponds to backscatter and $\phi = 225°$ corresponds to forward scattering (see Fig. 7).

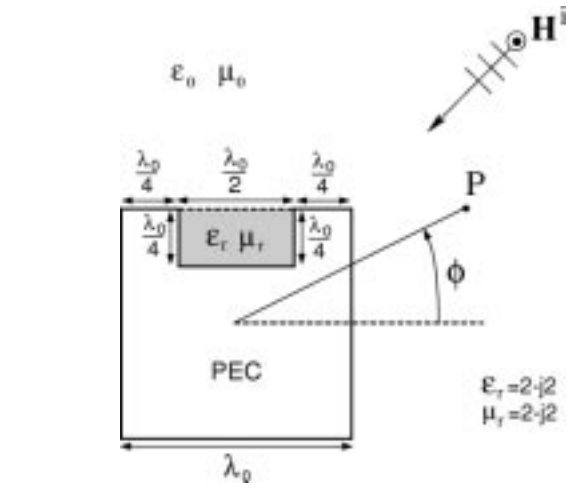

Fig. 7. Coated square cylinder with crack and illuminated by TE-polarized plane wave.

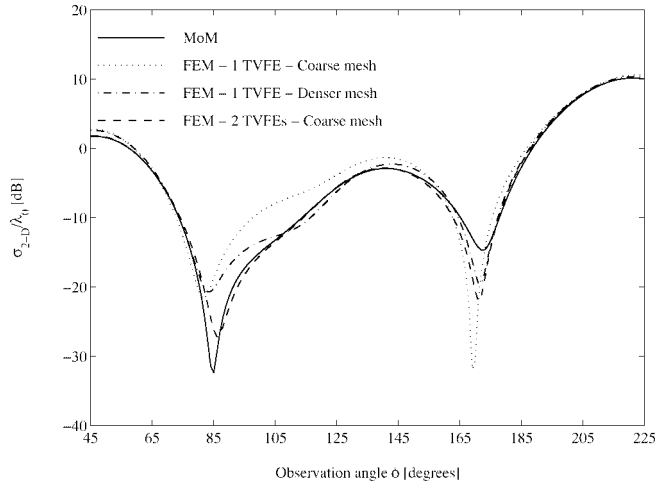

Fig. 8. Bistatic RCS of the cylinder in Fig. 7.

is denoted "FEM-2 TVFE's-coarse." For a mesh where the generic element edge size is $0.1\lambda_0$, the FEM result using the lowest order TVFE is denoted "FEM-1 TVFE-dense."

The "FEM-1 TVFE-coarse" result is seen to compare reasonably well with the exact MoM result. However, discrepancies can be seen and this is not surprising since the mesh is relatively coarse. For the denser mesh, the "FEM-1 TVFE-dense" result shows a slight improvement. However, by keeping the original mesh and employing the proposed mixed-order TVFE of order 1.5 close to the scatterer where the field can be expected to vary rapidly and accurate modeling is, therefore, necessary, the "FEM-2 TVFE's-coarse" result shows a significant improvement. It matches the MoM result exactly except in regions surrounding nulls and it was obtained using less computational resources (less unknowns, less nonzero matrix entries, and less matrix solution time) than the "FEM-1 TVFE-dense" result. In conclusion, we observe selective field expansion to be superior to the more traditional approach of using a denser mesh and the same TVFE throughout the computational domain.

We now consider a slightly different cylinder geometry by introducing a slab of length λ_0 and height $\lambda_0/4$ on top of the

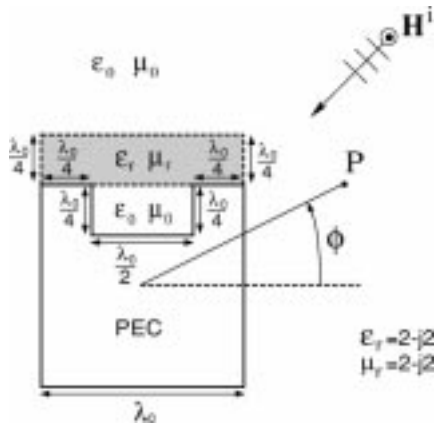

Fig. 9. Coated square cylinder with crack loaded by a dielectric slab and illuminated by TE-polarized plane wave.

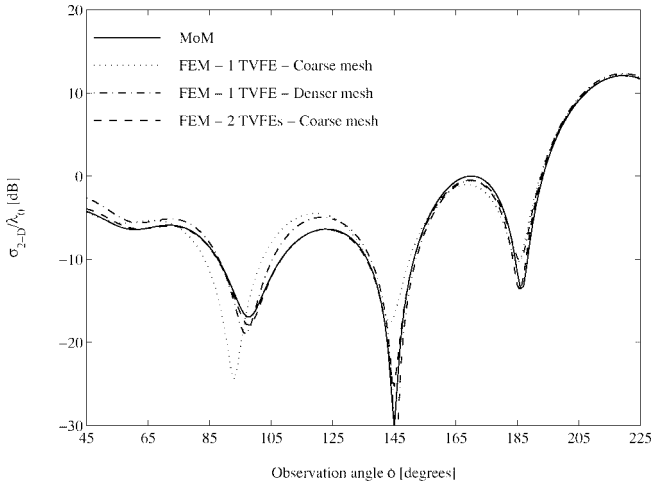

Fig. 10. Bistatic RCS of the cylinder in Fig. 9.

TABLE I
COMPARISON OF RELEVANT PARAMETERS FOR THE THREE FEM RESULTS IN FIG. 8

FEM Code	Unknowns	Non-zero mat. entries	Mat. solution time	RMS error
1 TVFE - Coarse mesh	811	3955	9 seconds	3.8657 dB
1 TVFE - Denser mesh	3977	19664	111 seconds	2.1059 dB
2 TVFEs - Coarse mesh	1070	7292	21 seconds	1.5614 dB

cylinder. As depicted in Fig. 9, the groove is filled with free space and the slab has the relative permittivity $\varepsilon_r = 2 - j2$ and the relative permeability $\mu_r = 2 - j2$. For the same illumination as before, results similar to those in Fig. 8 are given in Fig. 10 and they reinforce the conclusions from the previous case: the "FEM-1 TVFE-coarse" result compares reasonably well with the exact MoM result and the "FEM-2 TVFE's-coarse" result is, though found using less computational resources than the "FEM-1 TVFE-dense" result, significantly more accurate than the "FEM-1 TVFE-dense" result.

Explicit parameter values quantifying the computational savings for the results in Figs. 8 and 10 are given in Tables I and II, respectively. In both cases, improved accuracy is obtained for less nonzero matrix entries (i.e., less memory) and less solution time.

To test the validity of the reported observations for an alternative mesh truncation scheme, the FEM code was modified to

TABLE II
COMPARISON OF RELEVANT PARAMETERS FOR THE THREE FEM RESULTS IN FIG. 10

FEM Code	Unknowns	Non-zero mat. entries	Mat. solution time	RMS error
1 TVFE - Coarse mesh	900	4398	12 seconds	2.7353 dB
1 TVFE - Denser mesh	4469	22118	153 seconds	1.2883 dB
2 TVFEs - Coarse mesh	1280	9466	35 seconds	0.6290 dB

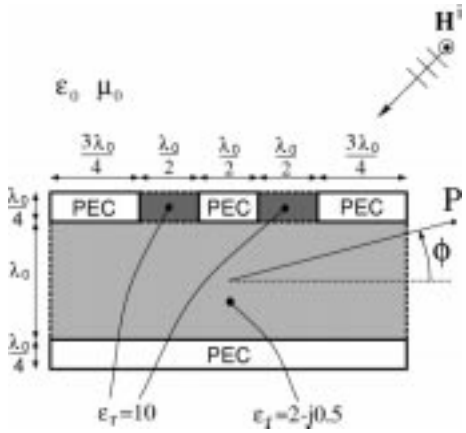

Fig. 11. Grating structure on top of a grounded dielectric and illuminated by TE polarized plane wave.

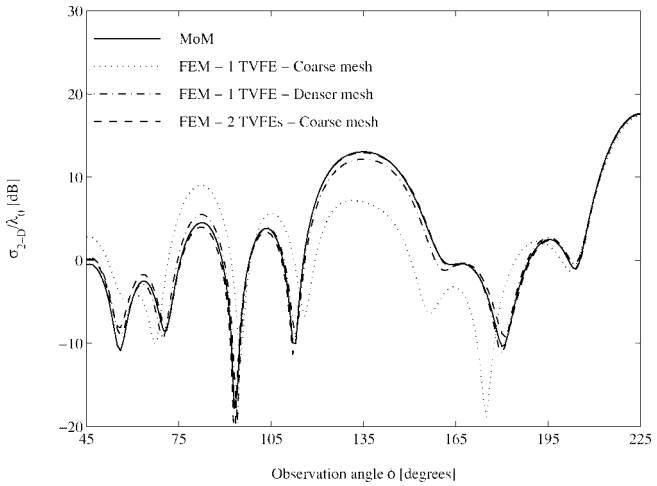

Fig. 12. Bistatic RCS of the cylinder in Fig. 11.

TABLE III
COMPARISON OF RELEVANT PARAMETERS FOR THE THREE FEM RESULTS IN FIG. 12

FEM Code	Unknowns	Non-zero mat. entries	Mat. solution time	RMS error
1 TVFE - Coarse mesh	1230	19662	172 seconds	5.3980 dB
1 TVFE - Denser mesh	2421	43961	301 seconds	0.9807 dB
2 TVFEs - Coarse mesh	1716	25884	534 seconds	0.7705 dB

use a boundary integral (BI) for truncating the finite-element mesh. Where the AA mesh truncation scheme is approximate, the BI is (at least until discretized and coupled with an FEM system) exact and, hence, it is attractive for truncating finite-element meshes. For our test, the integral contour is situated a slight distance away from the scatterer so that a piecewise constant (lowest order) expansion can be employed for discretizing the BI. As illustrated in Fig. 11, we consider a rectangular PEC cylinder of width $3\lambda_0$ and height $0.25\lambda_0$ covered by a dielectric material of width $3\lambda_0$ and height λ_0 whose relative permittivity is $\varepsilon_r = 2 - j0.5$. On top of the dielectric is a grating structure of height $0.25\lambda_0$ consisting of three PEC strips of lengths $0.75\lambda_0$, $0.5\lambda_0$ and $0.75\lambda_0$, respectively, separated by dielectric inserts of length $0.5\lambda_0$ having the relative permittivity $\varepsilon_r = 10$. A structure of this type (but of different size and different material composition) is of practical interest for guiding electromagnetic waves and below we demonstrate how a selective field expansion can lead to accurate modeling of the fields in and near the grating structure and thereby accurately predict the scattered field. The structure is situated in free space and illuminated as the previous two cylinders. Results similar to those in Fig. 8 and Table I are given in Fig. 12 and Table III. The results again reinforce the conclusions reported above, except that the matrix solution time for the "FEM-2 TVFE's-coarse" result is larger than that for the "FEM-1 TVFE-dense" result. This fact is due to the condition number of the resulting FEM-BI equation system and might change if a different iterative solver had been applied. Further, we note that the preprocessing time is significantly larger for the "FEM-1 TVFE-dense" result than the "FEM-2 TVFE's-coarse" result due to the larger BI system. This must be kept in mind when interpreting Table III.

We note that at least two other approaches could be utilized for improving the accuracy of FEM results. For example, higher order TVFE's (either Peterson's mixed-order TVFE of order 1.5 or the proposed mixed-order TVFE of order 1.5) could be applied throughout the computational domain. This approach was tested and the two mixed-order TVFE's of order 1.5 gave similar and accurate results but could not measure up with the selective approach in terms of computational resources. Alternatively, nonuniform meshing could be utilized. However, this could be employed for all the TVFE options described in this paper and was therefore not tested. Moreover, mesh regeneration for improved solution accuracy is not an attractive option. Nevertheless, it is reasonable to assume that this approach would lead to accurate results with a denser mesh close to the scatterer where the field is expected to vary rapidly.

V. CONCLUSIONS AND FUTURE WORK

We introduced a class of hierarchical TVFE's for FEM discretization. The properties of the proposed class of TVFE's were discussed and a comparison to those of traditional TVFE's was given. A set of numerical results were presented that demonstrate the effectiveness of the proposed class of hierarchical TVFE's when the computational domain is selectively discretized using the lowest order TVFE in part of the domain and a proposed hierarchical mixed-order TVFE of order 1.5 in the remaining part of the domain. Hence, the computational domain can initially be discretized using lowest order TVFE's and the accuracy of the solution can then be improved by selectively superimposing more vector basis functions where rapid field variation is anticipated, i.e., in regions near edges, near material boundaries, in dense dielectrics, etc.

Although the class of hierarchical TVFE's was presented for a triangular element, the approach has the potential to be more general. The derivation of a class of hierarchical

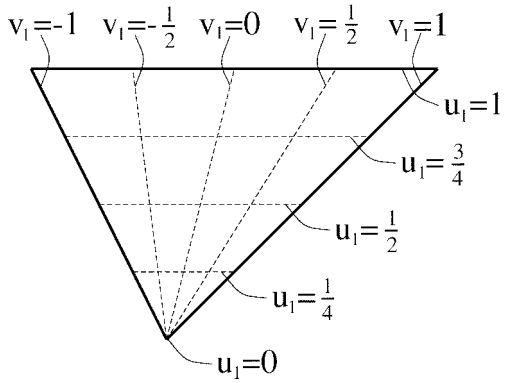

Fig. 13. Illustration of the variation of u_1 and v_1 over a triangle.

TVFE's for a generalized quadrilateral and, as a special case, a curved triangle would again begin with a suitable polynomial expansion for a surface current as presented by Popović and Kolundžija. Such elements conform well to almost all geometries and are thus attractive for FEM discretization. Hierarchical mixed-order TVFE's of order 0.5, 1.5, and 2.5 for a tetrahedral element have already been developed [24].

APPENDIX A

In this Appendix, explicit expressions for $\mathbf{W}_1$, $\mathbf{W}_2$, and $\mathbf{W}_3$ are derived.

To derive an expression for $\mathbf{W}_1$, we introduce two coordinates (u_1, v_1) over the triangle. These are degenerates of similar coordinates for a generalized quadrilateral [17]. u_1 takes its minimum value $u_{1,\min} = 0$ at node 1 and its maximum value $u_{1,\max} = 1$ along edge #2 while v_1 takes its minimum value $v_{1,\min} = -1$ along edge #3 and its maximum value $v_{1,\max} = 1$ along edge #1. u_1 is constant and v_1 is linear along straight lines parallel to edge #2 while u_1 is linear and v_1 is constant along straight lines starting at node 1 and ending at edge #2, as illustrated in Fig. 13. Using these coordinates, the position vector $\mathbf{r}$ defining P can be expressed as [17]

$$\mathbf{r} = \mathbf{r}_1 + u_1\mathbf{r}_{u_1} + u_1v_1\mathbf{r}_{u_1v_1} \tag{11}$$

where

$$\mathbf{r}_{u_1} = \tfrac{1}{2}[(\mathbf{r}_3 - \mathbf{r}_1) + (\mathbf{r}_2 - \mathbf{r}_1)] \tag{12}$$

$$\mathbf{r}_{u_1v_1} = \tfrac{1}{2}(\mathbf{r}_2 - \mathbf{r}_3). \tag{13}$$

Further, u_1 and v_1 can be shown to be related to the simplex coordinates ζ_1, ζ_2, and ζ_3 via

$$u_1 = \zeta_2 + \zeta_3 \tag{14}$$

$$v_1 = \frac{\zeta_2 - \zeta_3}{\zeta_2 + \zeta_3}. \tag{15}$$

From (4) for $n = 1$, trivial algebra then leads to

$$\mathbf{W}_1 = \zeta_2\nabla\zeta_3 - \zeta_3\nabla\zeta_2. \tag{16}$$

To derive expressions for $\mathbf{W}_2$ and $\mathbf{W}_3$, we can similarly introduce coordinates (u_2, v_2) and (u_3, v_3) where $v_{2,3} = \pm 1$ along the two edges shared by node 2, 3, $u_{2,3} = 0$ at node $2, 3$ and $u_{2,3} = 1$ at the edge opposite to node $2, 3$. The algebra is similar and we arrive at

$$u_2 = \zeta_3 + \zeta_1 \tag{17}$$

$$v_2 = \frac{\zeta_3 - \zeta_1}{\zeta_3 + \zeta_1} \tag{18}$$

$$\mathbf{W}_2 = \zeta_3\nabla\zeta_1 - \zeta_1\nabla\zeta_3 \tag{19}$$

$$u_3 = \zeta_1 + \zeta_2 \tag{20}$$

$$v_3 = \frac{\zeta_1 - \zeta_2}{\zeta_1 + \zeta_2} \tag{21}$$

$$\mathbf{W}_3 = \zeta_1\nabla\zeta_2 - \zeta_2\nabla\zeta_1. \tag{22}$$

APPENDIX B

In this Appendix, explicit expressions for the vector basis functions discussed in Section III are presented. The basis functions are not normalized.

A. Whitney's Mixed-Order TVFE of Order 0.5

Whitney's mixed-order TVFE of order 0.5 is characterized by the three vector basis functions

$$\mathbf{W}_1^1 = \zeta_2\nabla\zeta_3 - \zeta_3\nabla\zeta_2 \tag{23}$$

$$\mathbf{W}_2^1 = \zeta_3\nabla\zeta_1 - \zeta_1\nabla\zeta_3 \tag{24}$$

$$\mathbf{W}_3^1 = \zeta_1\nabla\zeta_2 - \zeta_2\nabla\zeta_1. \tag{25}$$

B. Peterson's Mixed-Order TVFE of Order 1.5

Peterson's mixed-order TVFE of order 1.5 is characterized by the eight vector basis functions

$$\mathbf{W}_1^2 = \zeta_2\nabla\zeta_3 \tag{26}$$

$$\mathbf{W}_2^2 = \zeta_3\nabla\zeta_2 \tag{27}$$

$$\mathbf{W}_3^2 = \zeta_3\nabla\zeta_1 \tag{28}$$

$$\mathbf{W}_4^2 = \zeta_1\nabla\zeta_3 \tag{29}$$

$$\mathbf{W}_5^2 = \zeta_1\nabla\zeta_2 \tag{30}$$

$$\mathbf{W}_6^2 = \zeta_2\nabla\zeta_1 \tag{31}$$

$$\mathbf{W}_7^2 = \zeta_3(\zeta_1\nabla\zeta_2 - \zeta_2\nabla\zeta_1) \tag{32}$$

$$\mathbf{W}_8^2 = \zeta_1(\zeta_2\nabla\zeta_3 - \zeta_3\nabla\zeta_2). \tag{33}$$

C. The Proposed Hierarchical Mixed-Order TVFE of Order 1.5

The proposed hierarchical mixed-order TVFE of order 1.5 is characterized by the eight vector basis functions

$$\mathbf{W}_1^3 = \zeta_2\nabla\zeta_3 - \zeta_3\nabla\zeta_2 \tag{34}$$

$$\mathbf{W}_2^3 = \zeta_3\nabla\zeta_1 - \zeta_1\nabla\zeta_3 \tag{35}$$

$$\mathbf{W}_3^3 = \zeta_1\nabla\zeta_2 - \zeta_2\nabla\zeta_1 \tag{36}$$

$$\mathbf{W}_4^3 = (\zeta_2 - \zeta_3)(\zeta_2\nabla\zeta_3 - \zeta_3\nabla\zeta_2) \tag{37}$$

$$\mathbf{W}_5^3 = (\zeta_3 - \zeta_1)(\zeta_3\nabla\zeta_1 - \zeta_1\nabla\zeta_3) \tag{38}$$

$$\mathbf{W}_6^3 = (\zeta_1 - \zeta_2)(\zeta_1\nabla\zeta_2 - \zeta_2\nabla\zeta_1) \tag{39}$$

$$\mathbf{W}_7^3 = \zeta_3(\zeta_1\nabla\zeta_2 - \zeta_2\nabla\zeta_1) \tag{40}$$

$$\mathbf{W}_8^3 = \zeta_1(\zeta_2\nabla\zeta_3 - \zeta_3\nabla\zeta_2). \tag{41}$$

D. Transformation Between Mixed-Order TVFE's of Order 1.5

The two mixed-order TVFE's of order 1.5 presented above are related through a linear transformation. Let $[\mathbf{W}_j^2]$ be a column vector containing Peterson's eight vector basis functions $\mathbf{W}_j^2$, $j = 1, \cdots, 8$, and $[\mathbf{W}_i^3]$ be a column vector containing the proposed eight vector basis functions $\mathbf{W}_i^3$, $i = 1, \cdots, 8$. In this case, $[\mathbf{W}_i^3]$ is related to $[\mathbf{W}_j^2]$ via

$$[\mathbf{W}_i^3] = [A_{ij}][\mathbf{W}_j^2], \tag{42}$$

where $[A_{ij}]$ is the sparse 8×8 transformation matrix

$$[A_{ij}] = \begin{bmatrix} 1 & -1 & 0 & 0 & 0 & 0 & 0 & 0 \\ 0 & 0 & 1 & -1 & 0 & 0 & 0 & 0 \\ 0 & 0 & 0 & 0 & 1 & -1 & 0 & 0 \\ 1 & 1 & 0 & 0 & 0 & 0 & -2 & -1 \\ 0 & 0 & 1 & 1 & 0 & 0 & 1 & -1 \\ 0 & 0 & 0 & 0 & 1 & 1 & 1 & 2 \\ 0 & 0 & 0 & 0 & 0 & 0 & 1 & 0 \\ 0 & 0 & 0 & 0 & 0 & 0 & 0 & 1 \end{bmatrix}. \tag{43}$$

E. The Proposed Hierarchical Mixed-Order TVFE of Order 2.5

The proposed hierarchical mixed-order TVFE of order 2.5 is characterized by the fifteen vector basis functions

$$\mathbf{W}_1^4 = \zeta_2 \nabla \zeta_3 - \zeta_3 \nabla \zeta_2 \tag{44}$$
$$\mathbf{W}_2^4 = \zeta_3 \nabla \zeta_1 - \zeta_1 \nabla \zeta_3 \tag{45}$$
$$\mathbf{W}_3^4 = \zeta_1 \nabla \zeta_2 - \zeta_2 \nabla \zeta_1 \tag{46}$$
$$\mathbf{W}_4^4 = (\zeta_2 - \zeta_3)(\zeta_2 \nabla \zeta_3 - \zeta_3 \nabla \zeta_2) \tag{47}$$
$$\mathbf{W}_5^4 = (\zeta_3 - \zeta_1)(\zeta_3 \nabla \zeta_1 - \zeta_1 \nabla \zeta_3) \tag{48}$$
$$\mathbf{W}_6^4 = (\zeta_1 - \zeta_2)(\zeta_1 \nabla \zeta_2 - \zeta_2 \nabla \zeta_1) \tag{49}$$
$$\mathbf{W}_7^4 = (\zeta_2 - \zeta_3)^2(\zeta_2 \nabla \zeta_3 - \zeta_3 \nabla \zeta_2) \tag{50}$$
$$\mathbf{W}_8^4 = (\zeta_3 - \zeta_1)^2(\zeta_3 \nabla \zeta_1 - \zeta_1 \nabla \zeta_3) \tag{51}$$
$$\mathbf{W}_9^4 = (\zeta_1 - \zeta_2)^2(\zeta_1 \nabla \zeta_2 - \zeta_2 \nabla \zeta_1) \tag{52}$$
$$\mathbf{W}_{10}^4 = \zeta_1(\zeta_2 \nabla \zeta_3 - \zeta_3 \nabla \zeta_2) \tag{53}$$
$$\mathbf{W}_{11}^4 = \zeta_2(\zeta_3 \nabla \zeta_1 - \zeta_1 \nabla \zeta_3) \tag{54}$$
$$\mathbf{W}_{12}^4 = \zeta_3(\zeta_1 \nabla \zeta_2 - \zeta_2 \nabla \zeta_1) \tag{55}$$
$$\mathbf{W}_{13}^4 = \zeta_1^2(\zeta_2 \nabla \zeta_3 - \zeta_3 \nabla \zeta_2) \tag{56}$$
$$\mathbf{W}_{14}^4 = \zeta_2^2(\zeta_3 \nabla \zeta_1 - \zeta_1 \nabla \zeta_3) \tag{57}$$
$$\mathbf{W}_{15}^4 = \nabla(\zeta_1 \zeta_2 \zeta_3). \tag{58}$$

REFERENCES

[1] J. P. Webb, "Edge elements and what they can do for you," *IEEE Trans. Magn.*, vol. 29, pp. 1460–1465, Mar. 1993.

[2] J. C. Nédélec, "Mixed finite elements in $\mathbb{R}^3$," *Numerical Math.*, vol. 35, pp. 315–341, 1980.

[3] ———, "A new family of mixed finite elements in $\mathbb{R}^3$," *Numerical Math.*, vol. 50, pp. 57–81, 1986.

[4] Z. J. Cendes, "Vector finite elements for electromagnetic field computation," *IEEE Trans. Magn.*, vol. 27, pp. 3958–3966, Sept. 1991.

[5] A. F. Peterson and D. R. Wilton, "A rationale for the use of mixed-order basis functions within finite element solutions of the vector Helmholtz equation," in *Proc. 11th Annu. Rev. Progress Appl. Computat. Electromagn.*, Monterey, CA, Mar. 1995, pp. 1077–1084.

[6] D. Sun, J. Manges, X. Yuan, and Z. J. Cendes, "Spurious modes in finite-element methods," *IEEE Antennas Propagat. Mag.*, vol. 37, pp. 12–24, Oct. 1995.

[7] A. F. Peterson and D. R. Wilton, "Curl-conforming mixed-order edge elements for discretizing the 2D and 3D vector Helmholtz equation," *Finite Element Software for Microwave Engineering*, T. Itoh, G. Pelosi, and P. P. Silvester, Eds. New York: Wiley, 1996, ch. 5, pp. 101–124.

[8] J. P. Webb and S. McFee, "The use of hierarchical triangles in finite-element analysis of microwave and optical devices," *IEEE Trans. Magn.*, vol. 27, pp. 4040–4043, Sept. 1991.

[9] J. P. Webb and R. Abouchacra, "Hierarchical triangular elements using orthogonal polynomials," *Int. J. Numerical Methods Eng.*, vol. 38, pp. 245–257, 1995.

[10] H. Whitney, *Geometric Integration Theory*. Princeton, NJ: Princeton Univ. Press, 1957.

[11] G. Mur and A. T. de Hoop, "A finite-element method for computing three-dimensional electromagnetic fields in inhomogeneous media," *IEEE Trans. Magn.*, vol. MAG-21, pp. 2188–2191, Nov. 1985.

[12] J.-F. Lee, D.-K. Sun, and Z. J. Cendes, "Full-wave analysis of dielectric waveguides using tangential vector finite elements," *IEEE Trans. Microwave Theory Tech.*, vol. 39, pp. 1262–1271, Aug. 1991.

[13] A. F. Peterson, "Vector finite element formulation for scattering from two-dimensional heterogeneous bodies," *IEEE Trans. Antennas Propagat.*, vol. 42, pp. 357–365, Mar. 1994.

[14] R. Graglia, D. R. Wilton, and A. F. Peterson, "Higher order interpolary vector bases for computational electromagnetics," *IEEE Trans. Antennas Propagat.*, vol. 45, pp. 329–342, Mar. 1997.

[15] C. Carrié and J. P. Webb, "Hierarchical triangular edge elements using orthogonal polynomials," in *Proc. IEEE Antennas Propagat. Soc. Int. Symp.*, Montréal, Canada, July 1997, vol. 2, pp. 1310–1313.

[16] J. P. Webb and B. Forghani, "Hierarchical scalar and vector tetrahedra," *IEEE Trans. Magn.*, vol. 29, pp. 1495–1498, Mar. 1993.

[17] B. D. Popović and B. M. Kolundžija, *Analysis of Metallic Antennas and Scatterers*. Stevenage, U.K.: IEE Press, 1994, vol. 38.

[18] B. M. Kolundžija and B. D. Popović, "Entire-domain Galerkin method for analysis of metallic antennas and scatterers," in *Proc. Inst. Elect. Eng.*, vol. 140, pt. H, pp. 1–10, Feb. , 1993.

[19] L. S. Andersen and J. L. Volakis, "A novel class of hierarchical higher order tangential vector finite elements for electromagnetics," in *Proc. IEEE Antennas Propagat. Soc. Int. Symp.*, Montréal, Canada, July 1997, vol. 2, pp. 648–651.

[20] S. M. Rao, D. R. Wilton, and A. W. Glisson, "Electromagnetic scattering by surfaces of arbitrary shape," *IEEE Trans. Antennas Propagat.*, vol. AP-30, pp. 409–418, May 1982.

[21] A. F. Peterson, private communication (e-mail), Aug. 1997.

[22] L. S. Andersen, "Summary of finite element method formulations for solution of two-dimensional bounded- and unbounded-domain electromagnetic problems," Internal Rep., Radiation Lab., Dept. Elect. Eng. Comput. Sci., Univ. Michigan, Fall 1996.

[23] Y. Saad, *Iterative Methods for Sparse Linear Systems*. Boston, MA: PWS Publishing Company, 1996.

[24] L. S. Andersen and J. L. Volakis, "Hierarchical tangential vector finite elements for tetrahedra," *IEEE Microwave Guided Wave Lett.*, vol. 8, pp. 127–129, Mar. 1998.

Lars S. Andersen (S'96) was born in Herning, Denmark, on August 13, 1971. He received the M.Sc. degree in electrical engineering from the Technical University of Denmark, Lyngby, Denmark, in 1995. He is currently working toward the Ph.D. degree at the Radiation Laboratory, Department of Electrical Engineering and Computer Science, University of Michigan under a fellowship from the Danish Research Academy.

While completing his thesis project at the Department of Electromagnetic Systems, Technical University of Denmark, he spent three months at the Department of Electrical and Computer Engineering, University of Texas at Austin, as a Research Scholar. His research interests include high-frequency techniques and all aspects of numerical electromagnetics.

John L. Volakis (S'77–M'82–SM'89–F'96), for photograph and biography, see this issue, p. 32.